Molecular Crystals and Liquid Crystals
Publication details, including instructions for authors and subscription information:
http://www.tandfonline.com/loi/gmcl16

Effect of Dopants on the Conductivity Anisotropy and AC Dynamic Scattering of Liquid Crystals

J. David Margerum [a], Hong Sup Lim [a], Paul O. Braatz [a] & Anna M. Lackner [a]

[a] Hughes Research Laboratories, Malibu, California, 90265

Version of record first published: 28 Mar 2007.

To cite this article: J. David Margerum, Hong Sup Lim, Paul O. Braatz & Anna M. Lackner (1977): Effect of Dopants on the Conductivity Anisotropy and AC Dynamic Scattering of Liquid Crystals, Molecular Crystals and Liquid Crystals, 38:1, 219-228

To link to this article: http://dx.doi.org/10.1080/15421407708084388

Mol. Cryst. Liq. Cryst., 1977, Vol. 38, pp. 219–228
© Gordon and Breach Science Publishers, Ltd., 1977
Printed in Holland

Effect of Dopants on the Conductivity Anisotropy and AC Dynamic Scattering of Liquid Crystals†

J. DAVID MARGERUM, HONG SUP LIM, PAUL O. BRAATZ, and ANNA M. LACKNER
Hughes Research Laboratories, Malibu, California 90265

(*Received October 19, 1976*)

The dynamic scattering (DS) characteristics and the conductivity anisotropy ratio ($R_\sigma = \sigma_{\|}/\sigma_{\perp}$) are shown to depend upon the structure and concentration of conductivity dopants as well as upon the structure of two nematic liquid crystals. For both a phenyl benzoate liquid crystal and for MBBA the ac threshold voltage (V_{th}) decreases with increasing R_σ, and the optical density of scattering at 30 V rms is directly proportional to R_σ. In each liquid crystal there is a linear relationship between V_{th}^{-2} and R_σ^{-1}, in agreement with the Carr–Helfrich theory.

INTRODUCTION

The dynamic scattering[1] (DS) behavior of a nematic liquid crystal under an applied electrical field depends upon its alignment by the field and the conduction of current through it as well as on other factors. Purified liquid crystals, to which dopants have not been added, have high resistivities and do not show dynamic scattering.[2] Conductivity anisotropy has been assumed to be important in DS-type effects,[3–5] and in the Carr–Helfrich[6,7] model it is a key factor in the formation of Williams domain[8] patterns. Numerous conductivity dopants have been used to obtain DS effects, and there have been many reports on the conductivity anisotropy ratio[9] ($R_\sigma = \sigma_{\|}/\sigma_{\perp}$) of various nematic liquid crystals. Frequently, R_σ has been assumed to be simply a property of the liquid crystal, and the conductivity dopant was often an unknown impurity. Several authors[10–13] reported a variety of R_σ values for N-(*p*-methoxybenzylidene)-*p*-butylaniline (MBBA) containing

---

† Presented at the Sixth International Liquid Crystal Conference, Kent, Ohio, August 1976.

different dopants but did not comment on the dopant effect. Chang[14] reported that the conductivity anisotropy of MBBA increases with decreasing radius of the halide ion in a series of three tetrapentylammonium halide dopants. He also observed that the maximum contrast ratio of DS obtainable with various dopants increased with the conductivity anisotropy. Barnik *et al.*[15,16] recently measured R_σ values and the threshold voltage (V_{th}) of electrohydrodynamic instability (Williams domains) for a number of dopants in different liquid crystals. They reported[16] that a two-dimensional threshold analysis[17,18] for MBBA gave an excellent correlation between theory and the experiment for plots of V_{th} versus R_σ. Surprisingly, they found that the same theoretical calculations for MBBA also fit the experimental points for two other liquid crystals, namely a mixture of azoxy compounds and a mixture of MBBA with EBBA (*p*-ethoxybenzylidene-*p*-*n*-butylaniline).

In this work we examine the effect of dopant structure and concentration on the conductivity anisotropy as well as on the dynamic scattering properties of a phenyl benzoate liquid crystal in cells with surface-parallel alignment. Some similar studies on MBBA are carried out for comparison purposes regarding the effect of the liquid crystal (LC) on these factors.

EXPERIMENTAL

Both MBBA (clpt. 46.2°) and a phenyl benzoate mixture designated as HRL-2N10 are used in this study. The latter is a four-component mixture of *p*-butylphenyl *p*-toluate, *p*-butoxyphenyl *p*-butoxybenzoate, *p*-butoxyphenyl *p*-hexyloxybenzoate and *p*-butoxyphenyl *p*-octyloxybenzoate in a weight ratio of 15:5:9:9, respectively. HRL-2N10 has a nematic range of about 20° to 55°, a dielectric anisotropy of $\Delta\varepsilon = (5.14 - 5.26) = -0.12$ (25°C, 500 Hz) and a birefringence of $\Delta n = 0.14$ (25°, 545 nm). Before adding dopants, the LC's are highly resistive, with $\rho_\perp > 1 \times 10^{11}$ ohm-cm for MBBA and $\rho_\perp > 3 \times 10^{11}$ ohm-cm for HRL-2N10 at 100 Hz. The following conductivity dopants are used after purification and drying: (1) tetrabutylammonium trifluoromethanesulfonate (TBATMS); (2) tetrabutylammonium tetrafluoroborate (TBATFB); (3) tetrabutylammonium perchlorate (TBAP); (4) tetrabutylammonium iodide (TBAI); (5) tetrabutylammonium chloride (TBAC); (6) tetraethylammonium bromide (TEAB); (7) tetrabutylammonium bromide (TBAB); (8) tetrabutylammonium tetraphenylboride (TBATPB); and (9) a redox dopant[19,20] mixture consisting of equimolar concentrations of the donor di-*n*-butylferrocene (DBF) and the acceptor (2,4,7-trinitro-9-fluorenylidene)malononitrile (TFM). The salt dopants were obtained commercially and are purified by standard techniques, except for TBATMS which is prepared[21] by reaction of trifluoromethanesulfonic acid and tetrabutylammonium bromide and is purified by recrystallization from water and drying. Commercial DBF and TFM were purified by vacuum distillation and recrystallization from acetonitrile, respectively.

The conductivity anisotropy is calculated from resistivity measurements at room temperature with a 100 μm thick cell in which the liquid crystal is aligned by a 7.5 kG magnetic field, using a readout with a lock-in amplifier (PAR-186) and a current-to-voltage converter (Keithley 427). The R_σ values are taken at 100 Hz, but the values are constant over a wide frequency range. Both the R_σ values and the DS behavior are compared at the same resistivity (e.g., $\rho_\perp = 1.0 \times 10^9$ ohm-cm) from data taken for several different concentrations of each dopant over a $\rho_\perp$ range of about 6×10^8 to 3×10^9 ohm-cm. The DS test cells are made with transparent electrodes (indium tin oxide rubbed to give surface–parallel alignment) using 12.7 μm thick Mylar spacers. The transmission of DS is measured in an optical system with a resolution of 20 lp/mm using collimated green light (centered at 525 nm). The V_{th} for DS is obtained by extrapolating the steep decrease of transmission back to 100% T. This is essentially the same as the threshold voltage for the formation of Williams domains. The scattering curves (where $\%S = 100 - \%T$) are obtained from slow scan increases of applied voltage at 30 Hz and 100 Hz (sinusoidal). The thresholds at 30 Hz are reported here because they are slightly lower for the samples with a resistivity of 1×10^9 ohm-cm.

RESULTS AND DISCUSSION

Effect of dopants on conductivity anisotropy

Typical results are shown in Figures 1, 2 and 3. These clearly show that the conductivity anisotropy ratio (R_σ) for both the ester liquid crystal and MBBA is highly dependent upon the structure and concentration of the dopants. Comparisons made at a given resistivity also show that the R_σ for a given dopant is different in the ester than in MBBA. For example, at $\rho_\perp = 10^9$ ohm-cm TBATMS, TBAI, TBAC and TBAB all have lower R_σ values in the ester than in MBBA, despite the fact that the ester (clpt. 55°) might be expected to have a higher order parameter at 25° than MBBA (clpt. 46°). Our comparisons are made at the same liquid crystal resistivity rather than at the same dopant concentrations because the dissociation constants of the various salts are not identical. The resistivity is an approximate measure of the concentration of ionic species present if the ionic mobilities of the different species are roughly the same.

Increased dopant concentration shows a rather large effect in some cases, particularly in the ester liquid crystal. The dopants with less solubility in the

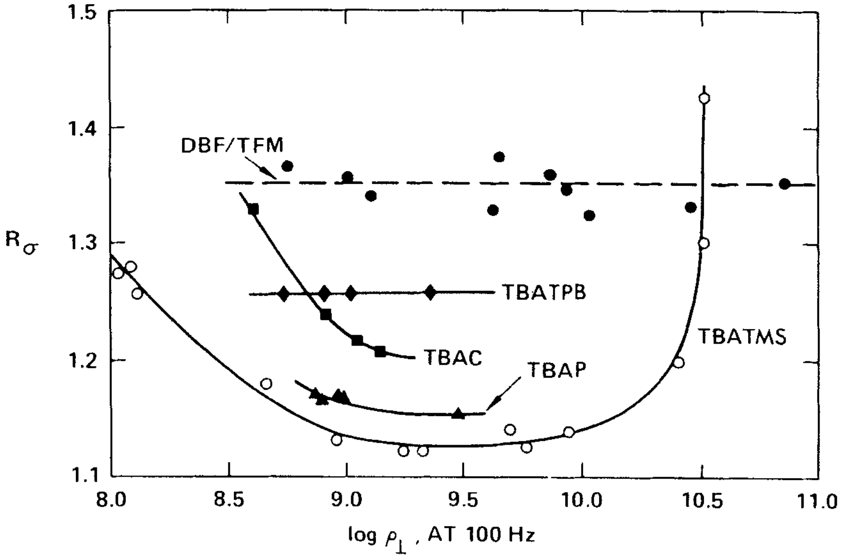

FIGURE 1 Conductivity anisotropy ratio of an ester liquid crystal containing different dopant structures and concentrations, ~25°C.

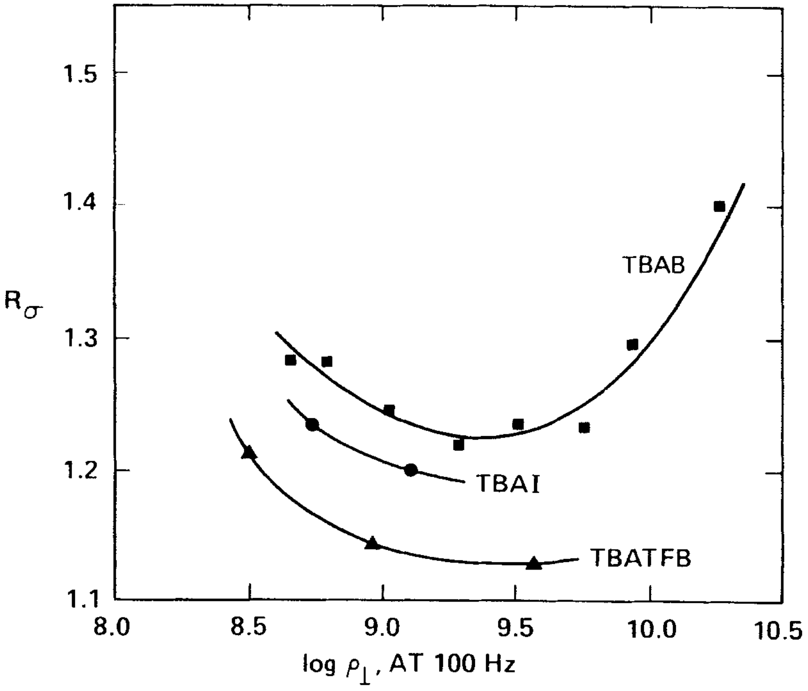

FIGURE 2 Conductivity anisotropy ratio of an ester liquid crystal containing different dopant structures and concentrations, ~25°C.

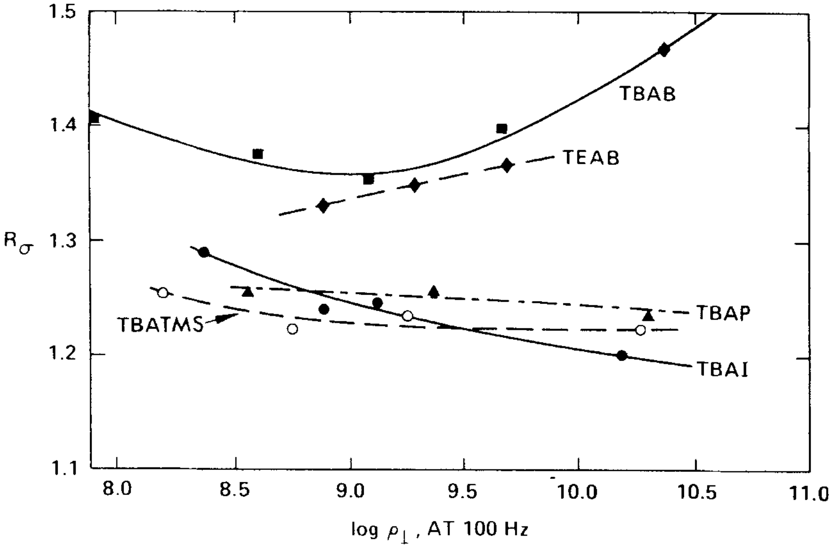

FIGURE 3 Conductivity anisotropy ratio of MBBA containing different dopant structures and concentrations, 25°C.

ester, such as TBAC and TBAB show the largest increases of R_σ at increased concentration (lower $\rho_\perp$). At high concentrations of 0.03 to 0.5% TBATMS shows a similar increase when $\rho_\perp < 10^9$ ohm-cm. Two of the more soluble dopants, TBATPB and DBF/TFM, show no significant variation of R_σ for the concentrations used. (Up to 0.5% of each redox dopant compound is used, and the conductive ions are presumably due to a small equilibrium concentration from: DBF + TFM = DBF^+ + TFM^-.) The salt dopants are more soluble in MBBA than in the ester, and as indicated in Figure 3 the R_σ values are less concentration-dependent. However, in MBBA they also show a general trend of higher R_σ values at increased dopant concentrations. We speculate that multiple ion association effects may occur as the salt concentrations approach saturation in the liquid crystal, where species such as ⊕⊖⊕, ⊖⊕⊖, etc., may be present and might contribute significantly to the conductivity anisotropy.

As noted by Chang,[14] the reproducibility of R_σ values is poor with different batches of MBBA, despite our method of handling the samples in a dry box flushed with nitrogen. The ester shows better reproducibility, although some dopants such as TBAB give more variable results than the others. We suspect some sort of impurity effects probably are responsible for the large deviations of R_σ at low concentrations ($\rho_\perp > 10^{10}$) of TBAB and TBATMS. Nevertheless, the R_σ values around $\rho_\perp = 10^9$ are fairly reproducible and comparisons can be made on the general effects of dopant structure. Our initial result with

TBATMS, TBATFB, TBAP, TBAI and TBAB in the ester seemed to support Chang's observations[14] that in MBBA smaller anions give larger R_σ values. However, this correlation does not hold up when we also consider the small Cl^- anion in TBAC and the large $(C_6H_5)_4B^-$ anion in TBATPB. Table I indicates that the R_σ data from Figures 1 and 2 do not correlate well with the crystallographic[22] sizes of anions. Other factors must be involved, such as ionic association, liquid crystal solvation, and the shape of the ions. For example, the flat shape and aromatic character of TFM^- anions may contribute to the large R_σ value of the DBF/TFM dopant. We plan to study such effects in more detail with other dopant and liquid crystal structures.

TABLE I

Comparison of relative anion sizes and R_σ values for TBA salts in an ester liquid crystal.

	R_σ Value[a] (increasing magnitude)		Anion size (crystallographic) (decreasing magnitude)
R_σ ↓	$CF_3SO_3^-$	Size ↑	$(C_6H_5)_4B^-$
	BF_4^-		$CF_3SO_3^-$
	ClO_4^-		ClO_4^-
	I^-		BF_4^-
	Cl^-		I^-
	Br^-		Br^-
	$(C_6H_4)_4B^-$		Cl^-

[a] At $\sigma_\perp = 10^{-9}$ ohm^{-1} cm^{-1} in HRL-2N10.

Effect of conductivity anisotropy on dynamic scattering (DS)

The DS behavior of a given liquid crystal is highly dependent upon the conductivity dopants used in it, as illustrated by the typical scattering versus voltage curves in Figure 4 for three different dopants in the HRL-2N10 ester liquid crystal. Scattering curves were taken for a total of eight dopants in the ester and for five dopants in MBBA. The experimental results of the DS threshold voltage (V_{th}) versus the conductivity anisotropy ratio (also at $\rho_\perp = 10^9$ ohm-cm) are shown in curves (a) and (b) of Figure 5. (Similar results were obtained at other resistivities.) Our DS comparisons are made at the same sample resistivities so that approximately equal current levels occur at the same applied voltage. It is apparent that each of these liquid crystals shows a distinctly different V_{th} versus R_σ curve, showing that V_{th} depends on the liquid crystal as well as the dopants. Of course, this is as we expected since the dielectric anisotropy of the ester ($\Delta\varepsilon = -0.12$) is much less negative than that of MBBA ($\Delta\varepsilon = -0.53$), the conductivity anisotropy of a given dopant is smaller in the ester than in MBBA, and the other material constants are probably different for the two liquid crystals.

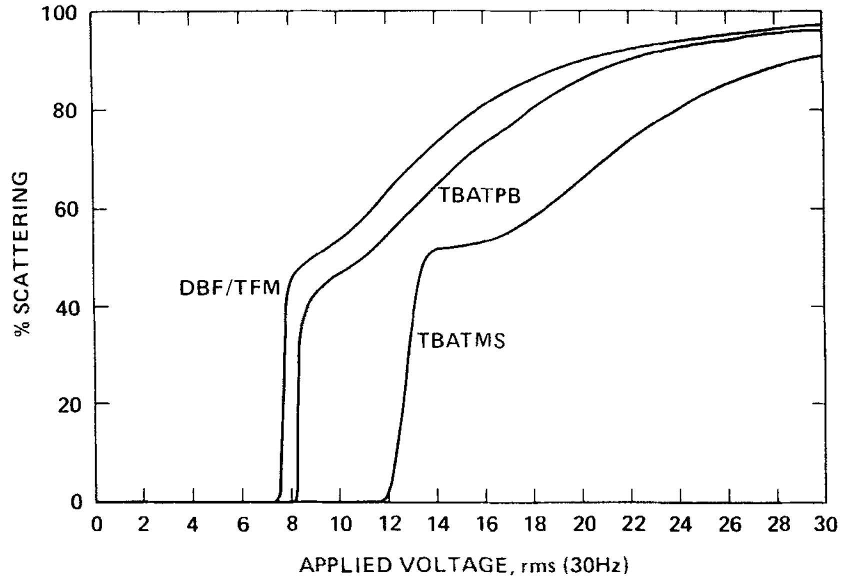

FIGURE 4 Typical dynamic scattering curves for dopants in an ester liquid crystal ($\rho_\perp$ = 1.0 × 10^9 ohm-cm, 12.7 μm thick cell spacers, surface-parallel alignment).

Helfrich[7] derived a one-dimensional expression for the dc threshold voltage of Williams domains in cells with surface-parallel alignment of liquid crystal. If the domain periodicity (λ) is included,[5] then the Helfrich is as follows:

$$V_{\mathrm{th}} = \pi\left(\frac{2d}{\lambda}\right)\left[\frac{k_{33}/\varepsilon_0}{\dfrac{\kappa_1\varepsilon_{\|}}{\eta_1}\left(\dfrac{\varepsilon_\perp}{\varepsilon_{\|}}-\dfrac{1}{R_\sigma}\right)+\dfrac{\Delta\varepsilon}{R_\sigma}}\right]^{1/2} \tag{1}$$

The expression for threshold voltage with low frequency ac excitation[23–25] contains extra terms of frequency dependence. The frequency dependence terms, however, drop out if $\omega^2/\omega_c^2 \ll 1$, where ω is the frequency of the applied ac-signal and ω_c is the cut-off frequency, i.e., the space charge-limited dielectric relaxation frequency. This frequency is proportional to the conductivity of LC.[5] Since the cut-off frequencies of the LC's used in the present studies are about 700 Hz at $\rho_\perp = 1 \times 10^9$ ohm-cm, the condition $\omega^2/\omega_c^2 \ll 1$ is satisfied at 30 Hz. Equation (1) and recent[26] values of physical constants for MBBA ($k_{33} = 8.11 \times 10^{-7}$ dyne, $\kappa_1 = 79.5$ cp, $\eta_1 = 104.5$ cp, $\varepsilon_{\|} = 4.72$, $\varepsilon_\perp = 5.25$) and a reported[27] experimental value of $\lambda = 1.3d$ (where d = cell thickness) are used to calculate curve (c) in Figure 5 for various values of R_σ. The refined two-dimensional models[16–18] give more accurate computer-calculated results for MBBA, but it can be seen that our results for MBBA

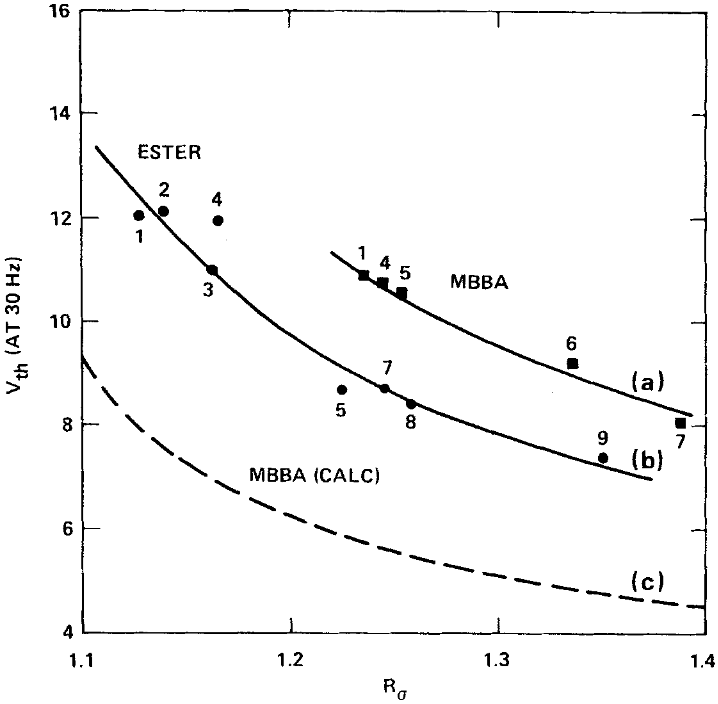

FIGURE 5 Effect of conductivity anisotropy ratio on dynamic scattering thresholds ($\rho_\perp$ = 1.0 × 10^9 ohm-cm, 12.7 μm thick spacer, surface-parallel alignment). Curve (a): experimental points for MBBA; curve (b): experimental points for HRL-2N10; curve (c): Helfrich equation calculation for MBBA. Dopants; 1 = TBATMS, 2 = TBATFB, 3 = TBAP, 4 = TBAI, 5 = TBAC, 6 = TEAB, 7 = TBAB, 8 = TBATPB, 9 = DBF/TFM.

(curve (a)) and the ester (curve (b)) are qualitatively similar to curve (c). This qualitative fit to the Helfrich equation is confirmed by the straight line relationships shown in Figure 6 for plots of V_{th}^{-2} versus R_σ^{-1}. Note that equation (1) can be rewritten as equation (2),

$$V_{th}^{-2} = A(R_\sigma^{-1}) + B \tag{2}$$

in which A and B are constants for a particular liquid crystal if we assume that the conductivity dopant concentrations are too small to affect the other physical constants.

The data in Figure 7 show that the optical density of scattering ($-\log T$) of each of the two liquid crystals at a high voltage (30 V) is directly proportional to its conductivity anisotropy with a particular dopant. This is not surprising when one observes the long gray scale region of the scattering curves in Figure 4 and notes that the relationship of V_{th} versus R_σ in Figure 5

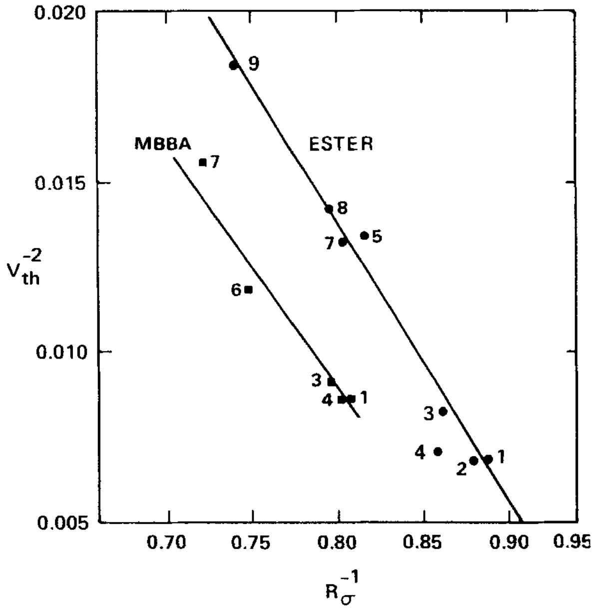

FIGURE 6 Helfrich equation plots for dynamic scattering threshold (same data and conditions as in Figure 5).

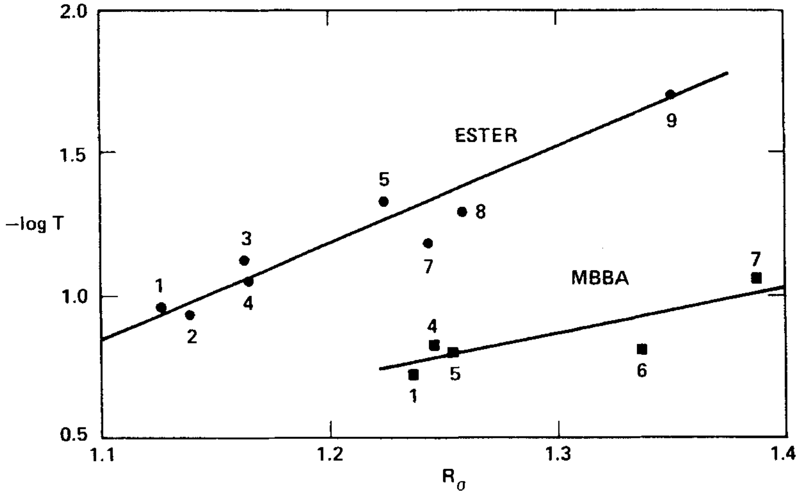

FIGURE 7 Effect of conductivity anisotropy ratio on the optical density of scattering at 30 V rms (same conditions as in Figure 5).

is not far from linear. In other words, it seems reasonable to us that the density of scattering is proportional to V/V_{th} and thus it is linear with R_σ, since we have found V_{th} to be approximately linear with R_σ.

Acknowledgment

We are indebted to the Directorate of Chemical Sciences, Air Force Office of Scientific Research, Contract F44620-72-C-0075 for partial financial support of this research, and to John E. Jensen and Deborah S. Smythe for assistance in preparing some of the samples.

References

1. G. H. Heilmeier, L. A. Zanoni, and L. A. Barton, *Appl. Phys. Lett.*, **13**, 46 (1968); *Proc. IEEE*, **56**, 1162 (1968).
2. G. H. Heilmeier, L. A. Zanoni, and L. A. Barton, *IEEE Trans. Elec. Dev.*, **ED-17**, 22 (1970).
3. P. A. Penz, *Phys. Rev. Lett.*, **24**, 1405 (1970).
4. P. G. De Gennes, *Comments Solid State Phys.*, **3**, 35 (1970).
5. T. J. Scheffer and H. Gruler, Electro-optics of liquid crystals, in *Molecular Electro-Optics*, C. T. O'Konski, ed. (Marcel Dekker, in press, 1976).
6. E. F. Carr, *Mol. Cryst. Liq. Cryst.*, **7**, 253 (1969).
7. W. Helfrich, *J. Chem. Phys.*, **51**, 4092 (1969).
8. R. Williams, *J. Chem. Phys.*, **39**, 384 (1963).
9. $R_\sigma = \sigma_\parallel/\sigma_\perp$, where $\sigma_\parallel$ and $\sigma_\perp$ are conductivities of the LC with its directors parallel and perpendicular to the electric field, respectively.
10. F. Rondelez, D. Diguet, and G. Durand, *Mol. Cryst. Liq. Cryst.*, **15**, 183 (1971).
11. G. J. Sprokel, *Mol. Cryst. Liq. Cryst.*, **22**, 249 (1973).
12. G. J. Sprokel, *Mol. Cryst. Liq. Cryst.*, **26**, 45 (1974).
13. R. Chang and J. M. Richardson, *Mol. Cryst. Liq. Cryst.*, **28**, 189 (1974).
14. R. Chang, in *Liquid Crystals and Ordered Fluids*, Vol. 2, J. F. Johnson and R. S. Porter, eds. (Plenum Publishing Corp., 1974), p. 367.
15. M. I. Barnik, L. M. Blinov, M. F. Grebenkin, S. A. Pikin, and V. G. Chigrinov, *Zh. Eksp. Teor. Fiz.*, **69**, 1080 (1975).
16. M. I. Barnik, L. M. Blinov, M. F. Grebenkin, S. A. Pikin, and V. G. Chigrinov, *Physics Lett.*, **51A**, 175 (1975).
17. S. A. Pikin, *Zh. Eksp. Teor. Fiz.*, **60**, 1185 (1971); *Sov. Phys.-JETP*, **33**, 641 (1971).
18. P. A. Penz and G. W. Ford, *Phys. Rev. A*, **6**, 414 (1972).
19. H. S. Lim and J. D. Margerum, *Appl. Phys. Lett.*, **28**, 478 (1976).
20. H. S. Lim and J. D. Margerum, *J. Electrochem. Soc.*, **123**, 837 (1976).
21. K. Ronseau, G. C. Farrington, and D. Dolphin, *J. Org. Chem.*, **37**, 3968 (1972).
22. K. H. Stern and E. S. Amis, *Chem. Rev.*, **59**, 164 (1959).
23. Orsay Liquid Crystal Group, *Phys. Rev. Lett.*, **25**, 1642 (1970).
24. Orsay Liquid Crystal Group, *Mol. Cryst. Liq. Cryst.*, **12**, 251 (1971).
25. E. Dubois-Violette, P. G. de Gennes, and O. Parodi, *J. Physique*, **32**, 305 (1971).
26. C. Z. van Doorn, *J. Appl. Phys.*, **46**, 3738 (1975).
27. D. Meyerhofer and A. Sussman, *Appl. Phys. Lett.*, **20**, 337 (1972).